Normalized p-y analysis method for laterally loaded piles in sand based on CPT results

Garam Kim / Primary author
School of Civil and Environmental Engineering, Yonsei University, Seoul, Republic of Korea, mil4u@yonsei.ac.kr

Incheol Kim[1], Jiyeong Lee[2], Qaisar Abbas[3]
School of Civil and Environmental Engineering, Yonsei University, Seoul, Republic of Korea, skah3000@yonsei.ac.kr[1], jyoung12@yonsei.ac.kr[2], abbasqaisar935@gmail.com[3]

Junhwan Lee / Corresponding author
School of Civil and Environmental Engineering, Yonsei University, Seoul, Republic of Korea, junlee@yonsei.ac.kr

ABSTRACT: A normalized *p-y* analysis method based on the CPT cone resistance is presented for estimating lateral displacements of piles embedded in sands. The method introduces and utilizes the continuous depth profile of soil condition and stress state directly using the CPT cone resistance, which enables more detailed and accurate estimation of lateral pile displacements. The non-linear characteristics of lateral load response were considered by introducing the hyperbolic relationship and used to normalize the *p-y* curve through the load transfer algorithm. The lateral soil resistance was obtained and expressed in terms of the cone resistance. Calculated lateral displacements of piles obtained using the CPT-based normalized *p-y* method were compared to those measured from the selected case example. Both lateral displacement and bending moment profiles were addressed and analyzed.

Keywords: *p-y* analysis, *p-y* curve, CPT, lateral displacement, laterally loaded pile

1. Introduction

For the design of a laterally loaded pile in sand, the *p-y* analysis method is often used to estimate the lateral displacement owing to the simplicity of the method and reasonableness of calculated results. In the *p-y* analysis, soils are modeled as a series of elastic springs where the non-linear characteristics between the soil reaction (p) and induced pile displacement (y) can be considered. The pile in this process is divided into several elastic elements [1, 2].

In the conventional *p-y* analysis, sampling and subsequent testing procedures are required in order to characterize the soil spring properties in the *p-y* curve analysis. This often results in unintended ignorance of the detailed and continuous depth profile of soil characteristics and stress state in the analysis [3]. For this reason, there have been several approaches, proposed to define the *p-y* analysis based on in-situ testing methods such as the pressuremeter test (PMT), dilatometer test (DMT), and cone penetration test (CPT) [4-6]. In particular, CPT is regarded as an effective option for pile lateral load analysis because the horizontal stress is a key component in both cone penetration and lateral load-carrying mechanisms [7, 8].

In the present study, the normalized *p-y* analysis method using CPT results in sands is presented based on the work and results of Kim et al. [6]. For the CPT-based *p-y* method, the cone resistance (q_c) is introduced into modeling the *p-y* curve to correlate the lateral load response of pile to lateral soil resistance. The detailed and continuous depth profile of soil characteristics can then be readily incorporated into the analysis through the values of q_c. Several case examples were selected and adopted to compare measured and predicted lateral displacements using the CPT-based normalized *p-y* analysis method.

2. Description of p-y curves in sands

The lateral load response of piles including the lateral displacement and mobilized bending moment can be analyzed using the beam-on-elastic foundation model where soils are assumed as a series of elastic springs characterized by *p-y* curves and pile segments [9]. For each pile segment, the equilibrium condition should be satisfied and the governing equation of the beam-on-elastic foundation model is given by:

$$E_p I_p \frac{d^4 y}{dz^4} + Q \frac{d^2 y}{dz^2} - p + W = 0 \qquad (1)$$

where E_pI_p = flexural rigidity of pile; Q = axial load; p = soil reaction per unit length; W = distributed load along pile; y = lateral displacement of pile; and z = depth below the ground surface. The soil spring stiffnesses given by the *p-y* relationship is included in Eq. (1) and updated through the iterative calculation procedure. For piles in sands, the *p-y* methods proposed by Reese et al. [2] and API [10] have been widely adopted [9, 10]. The *p-y* curves of Reese et al. [2] and API [10] are defined based on the strength parameter mainly with the internal friction angle (ϕ).

Reese et al. [2] proposed the *p-y* curve formulation shown in Fig. 1(a). The ultimate lateral soil resistance (p_u)

is mobilized at large displacement of 3/80 times pile diameter (D) and is defined as the smaller value obtained by the following equations:

$$p_{us} = A\gamma' z \begin{bmatrix} \dfrac{K_0 z \tan\phi \sin\beta}{\tan(\beta-\phi)\cos\alpha} \\ +\dfrac{\tan\beta}{\tan(\beta-\phi)}(D + z\tan\beta\tan\alpha) \\ +K_0 z\tan\beta(\tan\phi\sin\beta - \tan\alpha) + K_a D \end{bmatrix} \quad (2)$$

$$p_{ud} = A\gamma' zD\left[K_a(\tan^8\beta - 1) + K_0\tan\phi\tan^4\beta\right] \quad (3)$$

where A = non-dimensional model coefficients; γ' = effective unit weight of soil; D = pile diameter; z = depth; K_0 = coefficient of lateral earth pressure at rest; K_a = coefficient of active earth pressure; ϕ = internal friction angle of soil; $\alpha = \phi/2$; and $\beta = 45°+\phi/2$.

API [10] proposed the *p-y* curve function in the form of the hyperbolic tangent relationship given as follows:

$$p = Ap_u \tanh\left(\frac{kz}{Ap_u}y\right) \quad (4)$$

where A = non-dimensional model coefficients = $[3 - 0.8(z/D)] \geq 0.9$ for static loading and 0.9 for cyclic loading; p_u = ultimate lateral resistance; k = initial subgrade reaction modulus; and z = depth. The p_u is then given as the minimum of the followings:

$$p_u = (C_1 z + C_2 D)\gamma' z \quad (5)$$

$$p_u = C_3 D\gamma' z \quad (6)$$

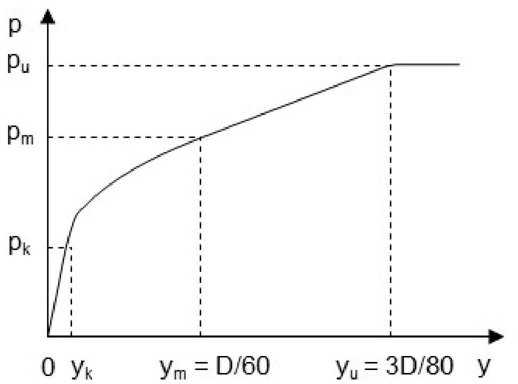

(a)

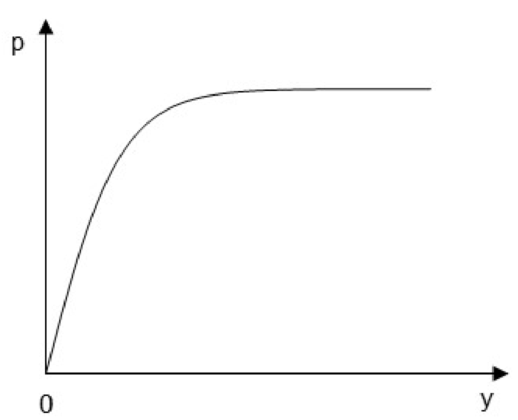

(b)

Figure 1. Existing p-y curves for sand: (a) Reese et al. [2]; and (b) API [10].

where C_1, C_2, and C_3 = model coefficients that are given as a function of internal friction angle. Fig. 1(b) shows the p-y curve of API [10].

3. CPT-based p-y curve for sands

In the conventional *p-y* methods, the limitation is inherent due to the use of simplified depth profiles caused by the soil sampling procedure and the assumption that soils are idealized with discrete springs defined by the *p-y* curves. The discontinuous condition of soil springs can be compensated by introducing the continuous CPT profile into *p-y* analysis [6]. Changes in soil and stress conditions can be reflected directly in the analysis by incorporating the cone resistance (q_c) into the *p-y* curve at a certain depth.

The hyperbolic function has been widely adopted in various geotechnical problems to describe the nonlinear stress-strain or load-displacement behavior of soil [11]. The hyperbolic function can also be applied to define the non-linear *p-y* curve in a normalized form given as follows [6]:

$$\frac{p}{p_u} = \frac{y/y_u}{a + b(y/y_u)} \quad (7)$$

where p = lateral soil resistance; p_u = ultimate lateral soil resistance; y = lateral displacement of pile; y_u = lateral displacement at the ultimate state; a = stiffness ratio = $E_{py,u}/E_{py,0}$; $E_{py,0}$ = initial stiffness on *p-y* curve; $E_{py,u}$ = *p-y* stiffness at the ultimate state = p_u/y_u.; and b = hyperbolic reduction factor. The stiffness ratio (a) is related to a strain at the ultimate state (ε_u) and can be obtained by the following relationship proposed by Kumar et al. [12].

$$a = 0.052\varepsilon_u^{-0.48} \quad (8)$$

The ε_u can be obtained from induced lateral displacement at the ultimate state (y_u). Blaney and O'Neil [13] presented the following relationship between ε_u and y_u:

$$\varepsilon_u = \frac{y_u}{1.667D} \quad (9)$$

where D = pile diameter. This leads that the value of a is equal to 0.321 from Eq. (8) by substituting y_u with $3D/80$ in Reese et al. [2]. The p_u is mobilized at y_u. This indicates that the normalized form of p/p_u is equal to unity when the ultimate state of y/y_u is equal to unity. From the relationship, b can be obtained as equal to 0.679. Equation (6) can then be rewritten as:

$$\frac{p}{p_u} = \frac{y/y_u}{0.321 + 0.679(y/y_u)} \quad (10)$$

The p_u is a key component in the lateral load response. p_u is the maximum resistance that can be mobilized for a given local soil condition, stress state and strength characteristic of the soil. The correlation of p_u and q_c was proposed by Lee at al. [14] given as follows:

$$p_u = 2.775D\,q_c^{0.391}\sigma'^{\,0.609}_m \quad (11)$$

where D = pile diameter; q_c = cone resistance; and σ'_m = mean effective stress. Note that the relationship between p_u and q_c of Eq. (11) corresponds to p_u in Broms [15] and was modified to match and compatible with the normalized *p-y* function. Therefore, Eq. (9) can be expressed as:

Table 1. Soil properties for *p-y* analysis at test site

Depth (m)	Soil type	Saturated unit weight, γ_{sat} (kN/m^3)	Friction angle, ϕ (°)		Lateral subgrade modulus, k (MN/m^3)		Undrained shear strength, s_u (kPa)	ε_{50}
			API method	Bolton method	API method	Bolton method		
0.0 - 0.5	Sand	19.5 (not saturated)	33	39	24.4	60.0	-	-
0.5 - 2.6	Sand	20.1	33	39	15.4	35.2	-	-
2.6 - 3.0	Sand	20.1	32	37	13.6	35.2	-	-
3.0 - 4.0	Sand	20.1	32	36	13.6	29.8	-	-
4.0 - 4.7	Sand	20.1	32	36	13.6	24.4	-	-
4.7 - 6.0	Sand	20.1	30	36	10.8	24.4	-	-
6.0 - 7.5	Sand	20.1	30	35	10.8	21.7	-	-
7.5 - 9.3	Soft clay	19.3	-	-	-	-	19.2	0.01
9.3 - 10.2	Sand	20.1	30	34	10.8	19.0	-	-
10.2 - 11.8	Soft clay	19.3	-	-	-	-	19.2	0.01

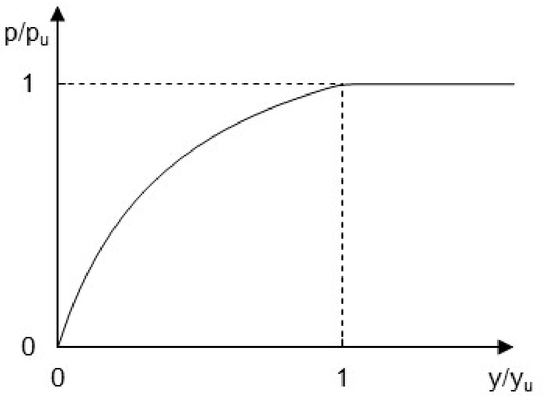

Figure 2. Normalized *p-y* curve based on CPT result for sand.

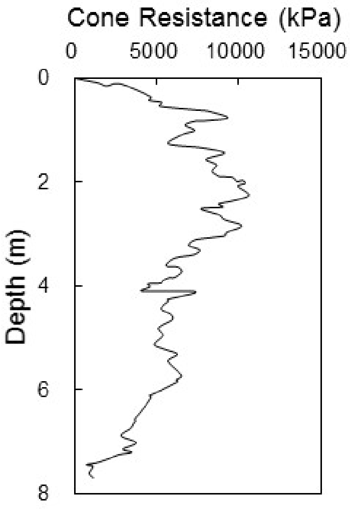

Figure 3. CPT profile at test site [16].

$$p = q_c^{\,0.391} \sigma_m'^{\,0.609} \frac{y}{0.00434 + 0.245(y/D)} \tag{12}$$

It is noted that the effect of the horizontal stress and its continuous profile on p_u is included in σ'_m and q_c whereas the nonlinearity in the load-displacement curve can be considered using the hyperbolic formulation of Eq. (12). Fig. 2 shows the CPT-based normalized *p-y* curve of Eq. (12).

4. Comparison with field load tests

To check the results of the CPT-based *p-y* method reviewed in this study, a case example was selected from the literature [16] and compared with the estimated results using the CPT-based method. The test pile was a steel pipe pile with an outside diameter of 0.324 m and a thickness of 0.01 m. The yield strength of the steel pipe was 404.6 MPa based on 2% offset criteria and the moment of inertia was 1.43×10^{-4} m^4. The yield bending moment was calculated to be 357.1 kN·m. The embedded length of the pile was 11.5 m and the lateral load was applied at 0.69 m above the ground surface.

The test site was located on Treasure Island in San Francisco Bay, US. The soil of the test site was sand to a depth of 7.5 m, and the clay layer existed from 7.5 m to 9.3 m below the ground surface. The upper sand layer was classified into SP, SP-SM, and SM according to the Unified Soil Classification System (USCS). The groundwater table was located about 0.5 m below the ground surface during the pile testing. The depth profile of q_c is shown in Fig. 3. The average values of q_c were in the range between 4 to 9 MPa in the upper sand layer.

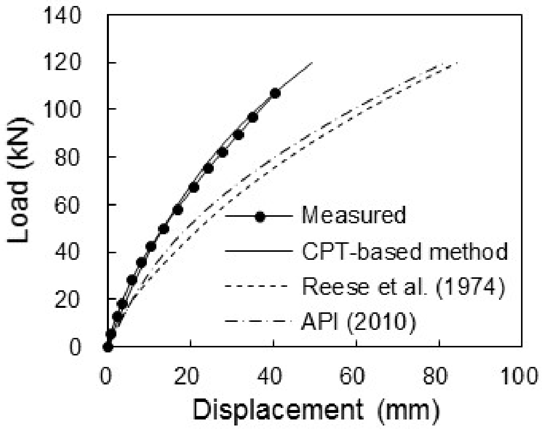

(a)

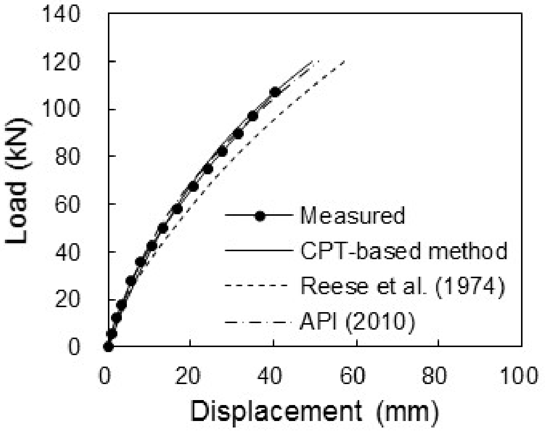

(b)

Figure 4. Lateral load-displacement curves using friction angle of (a) API [10]; and (b) Bolton [17].

The detailed soil variables for the test site were reported in Rollins et al. [16] and the summary of soil properties is given in Table 1. To determine ϕ at the test site, the methods proposed by Bolton [17] and API [10] were adopted. According to Bolton [17], ϕ can be obtained using the following dilatancy equations:

$$\phi_p = \phi_c + 3I_R \tag{13}$$

$$I_R = D_R\left[Q - \ln\left(\frac{100\sigma'_{mp}}{p_A}\right)\right] - R \tag{14}$$

where ϕ_p and ϕ_c = peak and critical-state friction angles; I_R = dilatancy index; D_R = relative density; p_A = 100 kPa; σ'_{mp} = mean effective stress; and Q and R = intrinsic soil variables. For the API method [10], the following equation is used to obtain the friction angle.

$$\phi = 16D_R^{\;2} + 0.17D_R + 28.4 \tag{15}$$

It was found that higher friction angles were estimated using the Bolton method than the API method.

For the selected example, the *p-y* analyses were performed using the methods of Reese et al. [2] and API [10] and using the CPT-based method of Eq. (12). The values of ϕ obtained from both Bolton method and API method were adopted as input variables for the *p-y* methods of Reese et al. [2] and API [10]. The CPT profile in Fig. 3 was input for the CPT-based *p-y* analysis.

The measured and predicted lateral load-displacement curves are shown in Fig. 4. The predicted result using the CPT-based *p-y* method was in close agreement with the measured curve. For the methods of Reese et al. [2] and API [10], the accuracy of the predicted results was dependent on the adopted values of ϕ. The ϕ using the Bolton method induced stiffer lateral load response due to higher ϕ. In this case example, ϕ from the Bolton method produced better accuracy for the measured results. It is noted that the selection of ϕ was not required for the CPT-based *p-y* method.

The measured and predicted maximum bending moment curves using the property- and CPT-based *p-y* methods are compared in Fig. 5. In the measured curve, the bending moment did not reach to yield point of the pile. The accuracies of the calculated maximum bending moments using the conventional property-based *p-y* curves were quite different depending on adopted values of ϕ. The results using ϕ of the API method were overestimated at higher load level while those using ϕ of the Bolton method were in good agreement with the measured curve. Note that such a tendency should be limited for the selected case and may become different if different soil condition is addressed. The estimated results using the CPT-based method matched well the measured curve.

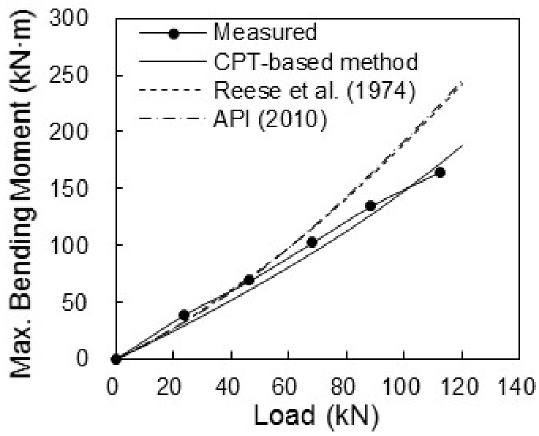

(a)

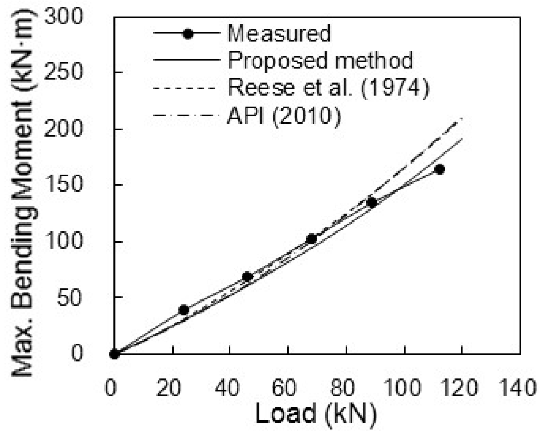

(b)

Figure 5. Maximum bending moments using friction angle of (a) API [10]; and (b) Bolton [17].

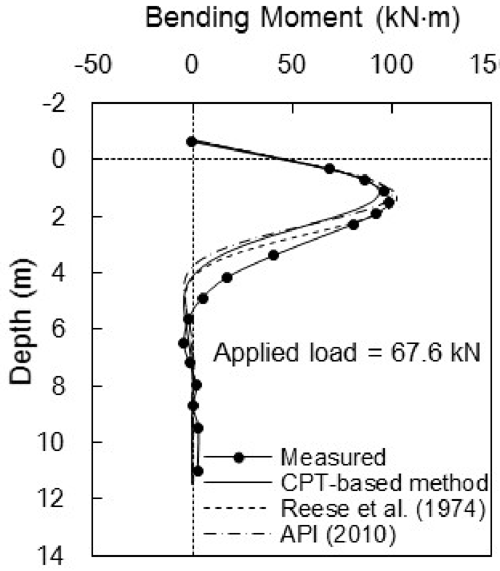

(a)

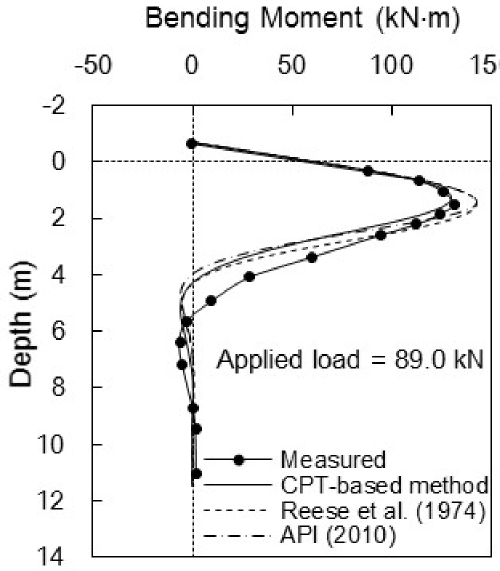

(b)

Figure 6. Depth profiles of bending moment at loading levels of (a) 67.6 kN; and (b) 89.0 kN.

The calculated bending moments along the depth were compared with the measured result. For methods proposed by Reese et al. (1974) and API (2010), the values of ϕ defined from both Bolton method were used. The results calculated using *p-y* curves were slightly different from those measured within a depth range of 3-6 m. For all *p-y* methods, the predicted depths corresponding to the maximum bending moments were in good agreement with the measured profile. For the applied load of 89.0 kN, the maximum bending moment estimated by CPT-based method was matched well with the measured value while property-based *p-y* methods overpredicted the results. Additionaly, it can be inferred from Fig. 5 that the property-based methods using ϕ obtained from API method would more overestimate the depth profile of bending moment.

5. Summary and conclusions

The CPT-based normalized *p-y* method was presented. The method takes advantage of CPT that is capable of measuring the cone resistance (q_c) with a continuous depth profile. To enhance the current *p-y* curve methods where detailed and continuous depth profile of in-situ soil condition is only limitedly considered, q_c was incorporated into the *p-y* curve function in a form of normalized relationship.

The CPT-based *p-y* curve for laterally loaded piles in sand was described based on the hyperbolic function with the nonlinear relationship between soil reaction and pile displacement. The ultimate lateral soil resistance (p_u) was considered as a key parameter in the *p-y* analysis, which was well correlated to q_c. The q_c-p_u correlation equation was then introduced into the displacement analysis where the depth profile of q_c is introduced directly as an input parameter.

The displacements and maximum bending moments were compared with the measured results for the case example to check the applicability of the method. The difference of results using CPT-based method from those using the conventional property-based methods was also presented. The CPT-based method provided the results in good agreement with the measured results without a selection process for the friction angle.

Acknowledgment

This work was supported by the Korea Institute of Energy Technology Evaluation and Planning (KETEP) and the Ministry of Trade, Industry & Energy (MOTIE) and the National Research Foundation of Korea (NRF) (Nos. 20194030202460 and 2020R1A2C2011966).

References

[1] Matlock, H., Reese, L. C. "Generalized solutions for laterally loaded piles", Journal of Soil Mechanics and Foundation, 86(5), pp. 63-91, 1960.

[2] Reese, L. C., Cox, W. R., Koop, F. D. "Analysis of laterally loaded piles in sand", In: Offshore Technology Conference, Houston, USA, 1974, pp. 473-485. https://doi.org/10.4043/2080-MS

[3] Pando, M. A., Ealy, C. D., Filz, G. M., Lesko, J. J., Hoppe, E. J. "A laboratory and field study of composite piles for bridge substructures", Federal Highway Administration, Washington, D. C., USA, Rep. FHWA-HRT-04-043, 2006.

[4] Robertson, P. K., Davis, M. P., Campanella, R. G. "Design of laterally loaded driven piles using the flat dilatometer", Geotechnical Testing Journal, 12(1), pp. 30-38, 1989.

[5] Gabr, M. A., Lunne, T., Powell, J. J. "P-y analysis of laterally loaded piles in clay using DMT", Journal of Geotechnical Engineering, 120(5), pp. 816–837, (1994). https://doi.org/10.1061/(ASCE)0733-9410(1994)120:5(816)

[6] Kim, G., Kyung, D., Park, D., Lee, J. "CPT-based py analysis for mono-piles in sands under static and cyclic loading conditions", Geomechanics and Engineering, 9, pp. 313-328, 2015. https://doi.org/10.12989/gae.2015.9.3.313

[7] Schnaid, F., Houlsby, G. T. "An assessment of chamber size effects in the calibration of in situ tests in sand", Géotechnique, 41(3), pp. 437-445, 1991. https://doi.org/10.1680/geot.1991.41.3.437

[8] Lee, J. H., Salgado, R. "Determination of pile base resistance in sands", Journal of Geotechnical and Geoenvironmental Engineering, 125(8), 673-683, 1999. https://doi.org/10.1061/(ASCE)1090-0241(1999)125:8(673)

[9] Reese, L. C., Van Impe. W. F. "Single Piles and Pile Groups Under Lateral Loading", A. A. Balkema, Rotterdam, Netherlands, 2001.
[10] API "Recommended Practice for Planning, Designing and Constructing Fixed Offshore Platforms - Working Stress Design", 21st edition, API Publishing Services, Washingto, D. C., 2010.
[11] Kondner, R. L. "Hyperbolic stress-strain response of cohesive soils", Journal of the Soil Mechanics and Foundations Division, 89(1), pp. 115-143, 1963.
[12] Kumar, S., Lalvani, L., Omar, M. "Nonlinear response of single piles in sand subjected to lateral loads using k_{hmax} approach", Geotechnical and Geological Engineering, 24(1), pp. 163-181, 2006. https://doi.org/10.1007/s10706-004-2760-4
[13] Blaney, G. W., O'Neill, M. W. "Measured lateral response of mass on single pile in clay", Journal of Geotechnical Engineering, 112(4), pp. 443–457, 1986. https://doi.org/10.1061/(ASCE)0733-9410(1986)112:4(443)
[14] Lee, J., Kim, M., Kyung, D. "Estimation of lateral load capacity of rigid short piles in sands using CPT results", Journal of Geotechnical and Geoenvironmental Engineering, 136(1), pp. 48-56, 2010. https://doi.org/10.1061/(ASCE)GT.1943-5606.0000199
[15] Broms, B. B. "Lateral resistance of piles in cohesionless soils", Journal of the Soil Mechanics and Foundations Division, 90(3), pp. 123–158, 1964.
[16] Rollins, K. M., Lane, J. D. Gerber, T. M. "Measured and computed lateral response of a pile group in sand", Journal of Geotechnical and Geoenvironmental Engineering, 131(1), pp. 103-114, 2005. https://doi.org/10.1061/(ASCE)1090-0241(2005)131:1(103)
[17] Bolton, M. D. "The strength and dilatancy of sands", Géotechnique, 36(1), pp. 65–78, 1986.